

Meson Shells

Paolo Palazzi

Abstract

An indication that mesons are organized in shells, originally expressed with masses, is converted into number of constituents using a mass unit obtained from a mass multiplicity analysis. Mesonic and nuclear shells are found to be structurally similar, with the main meson shell progression extending up to shell 8 and correlated with the quark composition, and no states beyond the 8th shell. Meson states corresponding to the doubly-magic nuclei are identified up to the 3rd shell, and in this sequence no states are present for shells 4 and above, as is the case for nuclei. In this context, the quantization of the meson mass unit suggests that mesons are solid-phase FCC aggregates of spin 1/2 partons of charge 0, +1 and -1, arranged with anti-ferromagnetic spin coupling in a variety of charge configurations related to J^{PC} and the quark composition. This hypothesis is confirmed by the sharper shell pattern obtained with η states. These results are used to formulate the ingredients of a shell model for mesons. In the emerging picture the number of parameters is considerably reduced in comparison with the standard model.

Address correspondence to: pp@particlez.org

Download from: <http://particlez.org/p3a/>

Table of Contents

1. Introduction ..	2
2. Particle shells ..	3
3. Mass unit ..	4
4. Meson shells and mass unit ..	5
5. From the Segrè plot to nuclear stability lines ..	6
6. Meson stability ..	7
1. The whole spectrum ..	7
2. Light unflavored mesons and strange mesons ..	8
7. U-grid, FCC lattice and η shells ..	9
8. Meson Shells, the full picture ..	10
9. Summary of results ..	11
10. Discussion ..	11
1. Ingredients for a model of mesons ..	12
2. Beyond the standard model? ..	12
Appendices	
A. The FCC nuclear model ..	13
B. Data and Statistics ..	14
Bibliography ..	14
Acknowledgements ..	14
Revision Record ..	14

Copyright © Paolo Palazzi, 2005

All rights reserved. Permission to use, copy, and distribute this document in its integrality in any medium for any purpose is hereby granted, provided that the contents are not modified in any way and that it is distributed free of charge. For anything else, please contact the author.

1. Introduction

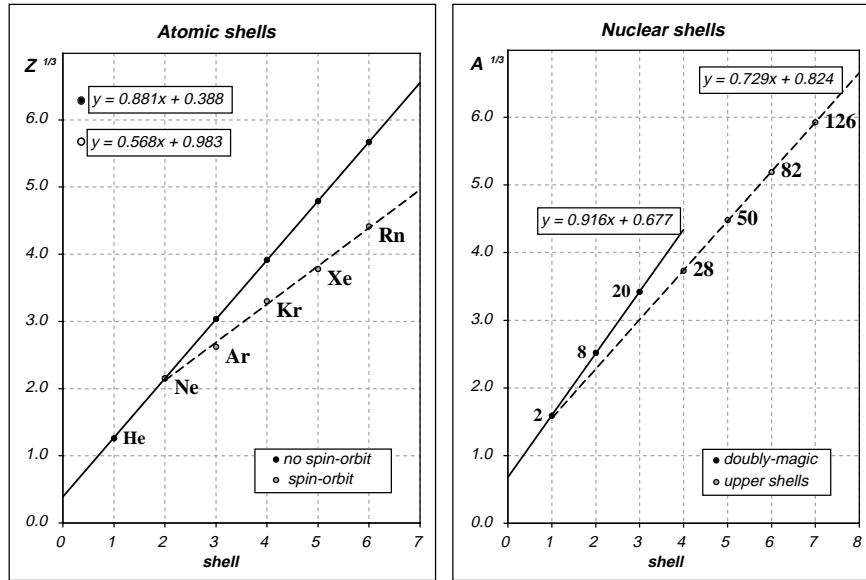
Quarks and their mixing are the cornerstone of particle physics. Essential to the understanding of decays, they are also the basis for the arrangement of mesons and baryons in SU(3) multiplets. Much in the same way, the chemical bond explains the interaction of atoms and their classification in the periodic table of the elements. Initially believed to be proportional to the weight, the bond was later recognized as a discrete attribute of atoms, and in the end understood as a combinatorial property of the electrons of the outer shell.

Following the original formulation of the quarks – and of the hypothesis that they might correspond to real constituents – in the early days a number of experiments were performed in the hope of detecting them, and none was successful. In spite of their elusiveness, quarks were nonetheless assumed to be real particles, identical with the partons seen in deep-inelastic scattering experiments. This conjecture was validated by a number of indirect experimental confirmations, and expressed within QCD, a theoretical framework describing also the undetectability of the quarks. On the other hand, the sequence of the estimated values of quark masses is a mystery, and up to now all attempts to compute the hadron masses for more than a handful of states at best have not been successful.

The present author addresses the crucial problem of hadron masses from a different angle, following a data-driven approach. The full spectrum of masses, lifetimes and quantum numbers of all the particles is analyzed statistically, in an attempt to extract yet-undetected features and regularities, and strengthen some that are already published but not widely known. The results are then interpreted bottom up, disregarding the fact that preliminary conclusions may appear to clash with established paradigms.

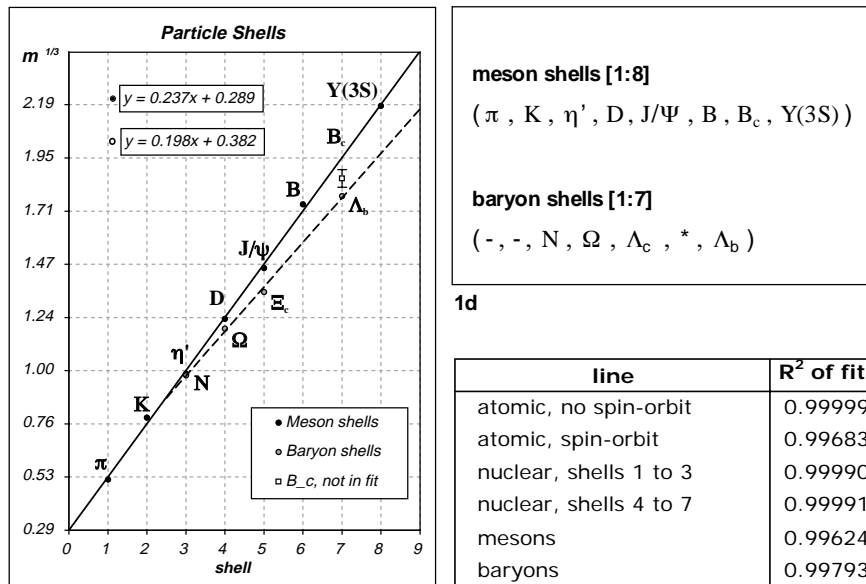
The hope is that, through this detour, the quarks may be expressed as collective properties of the partons in the context of a different model with different constituents, while preserving the concept of quarks as taxonomic and valence properties. For this attempt to be successful, the various experimental validations of quarks as constituents must be convincingly re-interpreted, and the rationale for the current estimated values of the quark masses also understood.

The present article is the third in a series. In the first one, "Particles and Shells" [1], indications of a shell organization of mesons and baryons were deduced from a stability analysis of the whole mass spectrum. The second paper, "Patterns in the Meson Mass Spectrum" [3], is a statistical analysis of the masses of all the mesons, validating the assumption that masses are multiples of a mass unit, and showing evidence of a second quantization. Here the results of [1] and [3] are combined, found to be mutually reinforcing, and used to formulate the ingredients for a shell model of mesons.



1a

1b



1c

1d

line	R ² of fit
atomic, no spin-orbit	0.99999
atomic, spin-orbit	0.99683
nuclear, shells 1 to 3	0.99990
nuclear, shells 4 to 7	0.99991
mesons	0.99624
baryons	0.99793

Fig. 1. Stability line plots from [1]: 1a, atomic shells; 1b, nuclear shells; 1c, particle shells; 1d, meson and baryon shells sequences; 1e, R² of line fits.

2. Particle shells

An indication that particles may be organized in shells was previously presented by this author on the basis of a stability analysis of the particle spectrum [1]. In this approach a generic 3D shell sequence is represented by a stability line connecting the cube roots of the total number of constituents of subsequent closed shell configurations, as verified in atoms and nuclei (figures 1a and 1b respectively). The analysis of hadrons identifies similar alignments with the cube root of the masses, reproduced in figure 1c.

Assuming only that each constituent ("parton" hereafter) contributes a constant amount to the total mass of the particle, the regular spacing shown in the mass stability lines of mesons and baryons at figure 1c would be a strong indication that the particles themselves have some form of shell structure. This is manifestly incompatible with the prevalent view that the partons are the quarks. Meson and baryon shells are organized along two different lines, and in order to relate line parameters to parton numbers the known masses must be converted into number of partons.

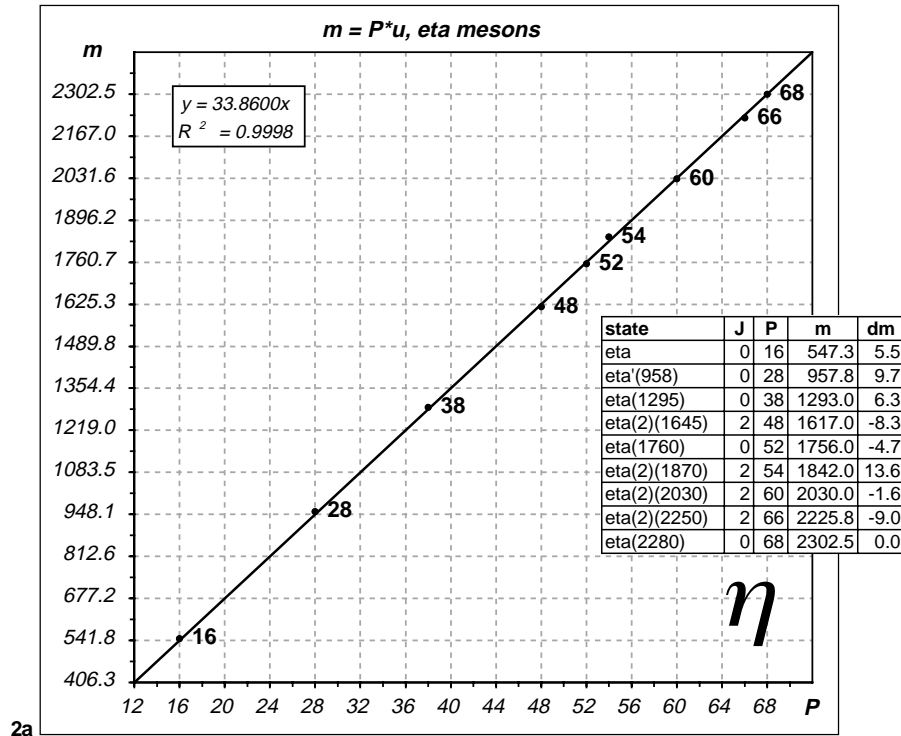
It is worth examining the parameters of the atomic and nuclear stability lines: the atomic line has an intercept of 0.39, while the nuclear lines corresponding to the lower and upper ranges of neutron magic numbers show intercepts of 0.68 and 0.82, about twice as much. In fact the first atomic shell has 2 electrons while the first nuclear shell consists of 4 nucleons, and the cube root of the count of these kernel configurations set the ordinate of the stability line at shell 1.

The properties of the interaction determine the configurations of the possible bound states with various number of components, and establish the growth rate from one shell to the next. For a central long-range interaction, such as in atoms, the solution of the bound state equation identifies subsequent closed shell configuration and determines the parameters of the line as in figure 1a, non spin-orbit. Spin-orbit coupling reduces the slope as in figure 1a spin-orbit. In nuclei stability is related to the magic numbers series separately for protons and for neutrons, however, with a sequence based on the atomic number $A = Z + N$, stability and spin-orbit coupling emerge in a similar way (figure 1b).

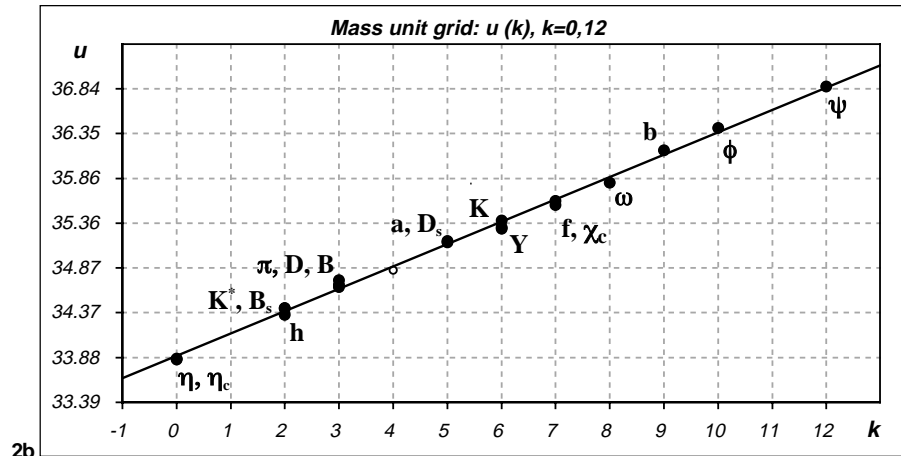
Conversely, for a given stability line such as the one of mesons in figure 1c, the values of the line parameters can give indications on the aggregation pattern and the interaction that produces it, provided that masses are converted to number of constituents.

The R² correlation coefficient for the linear fits is defined in appendix A. Table 1e lists the values of this parameter for the line fits of figures 1a, 1b and 1c.

The work presented here focuses on the mesons. The equivalent analysis for the baryons, currently in progress, will be published separately.



2a



2b

Fig. 2. Meson mass multiplicity: 2a, mass multiplicity assignment P for all η mesons listed by the PDG, and fit of the mass unit; 2b, u-grid: quantization of the mass unit for all meson families (both plots are reproduced from [3], the eta states table has been simplified).

3. Mass unit

The dominant hypothesis concerning particle masses is that quarks, well established as valence properties, are also the real constituents. If mesons are quark-antiquark states, then heavier mesons are bound states of heavier quarks. On the other hand, if stability is related to shells, and if it shows up in the mass spectrum, then the heavier states are simply built with more constituents, each bringing a fixed amount to the total mass. The two views are incompatible.

The concept that the masses of all the particles might be multiples of a single mass unit was proposed by Y. Nambu [2] in 1952 on the basis of the few states known at that time. It has been reformulated independently by various authors who found it statistically significant, but their results are seldom quoted (a more detailed account can be found in reference [3]).

Nambu's original conjecture was that $1/2$ of the π mass, about $70 \text{ MeV}/c^2$, is a significant mass unit. On this basis he then attributed to all known particles a "mass number", integer or half-odd: 0 for the photon, $3/2$ for the μ , 2 for the π , 7 for the K, $27/2$ for the nucleon and so on. Deviations from the rule are of the order of $\pm 1/10$ of the mass unit, moreover:

- the mass unit agrees with Heisenberg's natural unit m_e/α ($= 70.02 \text{ MeV}/c^2$);
- bosons have integer, while fermions half-integer, mass number;
- the electron mass and the $\pi^\pm - \pi^0$ mass difference correspond to a kind of fine structure.

Nambu stated also that his hypothesis was a "perhaps too ambitious and rather unsound" [attempt] "to look for an empirical "Balmer's law"". In the same spirit the present author is in the process of re-assessing this hypothesis on all particles listed by the PDG. The mass unit used is $u \approx 70/2 = 35 \text{ MeV}/c^2$, with mass numbers P (for parton) being odd for fermions and even for bosons. Some results of this analysis, based largely on automatic procedures and using no physics hypothesis whatsoever, have been published in [3] and show that:

- $m_i = P_i * u$, $u = 34.83 \text{ MeV}$ for all particles with mass $< 1 \text{ GeV}/c^2$, with p-value = 0.97 (see appendix B for the definition of p-value);
- $m_i = P_i * u_i$, [P even and u_i close to $35 \text{ MeV}/c^2$] for all known mesons, when grouped in families according to their PDG q-qbar assignment, I and J^{PC} , with p-value > 0.95 ; e.g. for the η family (figure 2a) $u_i = 33.86$ with p-value. = 0.999;
- the mass units u_i for the various families are quantized on a grid of 13 values [p-value. = 0.95], and their position on the grid shows intriguing correlations of J^{PC} for q-qbar symmetric vs q-qbar asymmetric meson types (figure 2b).

The open point at $k=4$ on the line in figure 2b is the mass unit of the unstable leptons also analyzed in [3]; (the equivalent analysis for baryons is in progress and the outcome is similar, apart from a more limited span of the mass units).

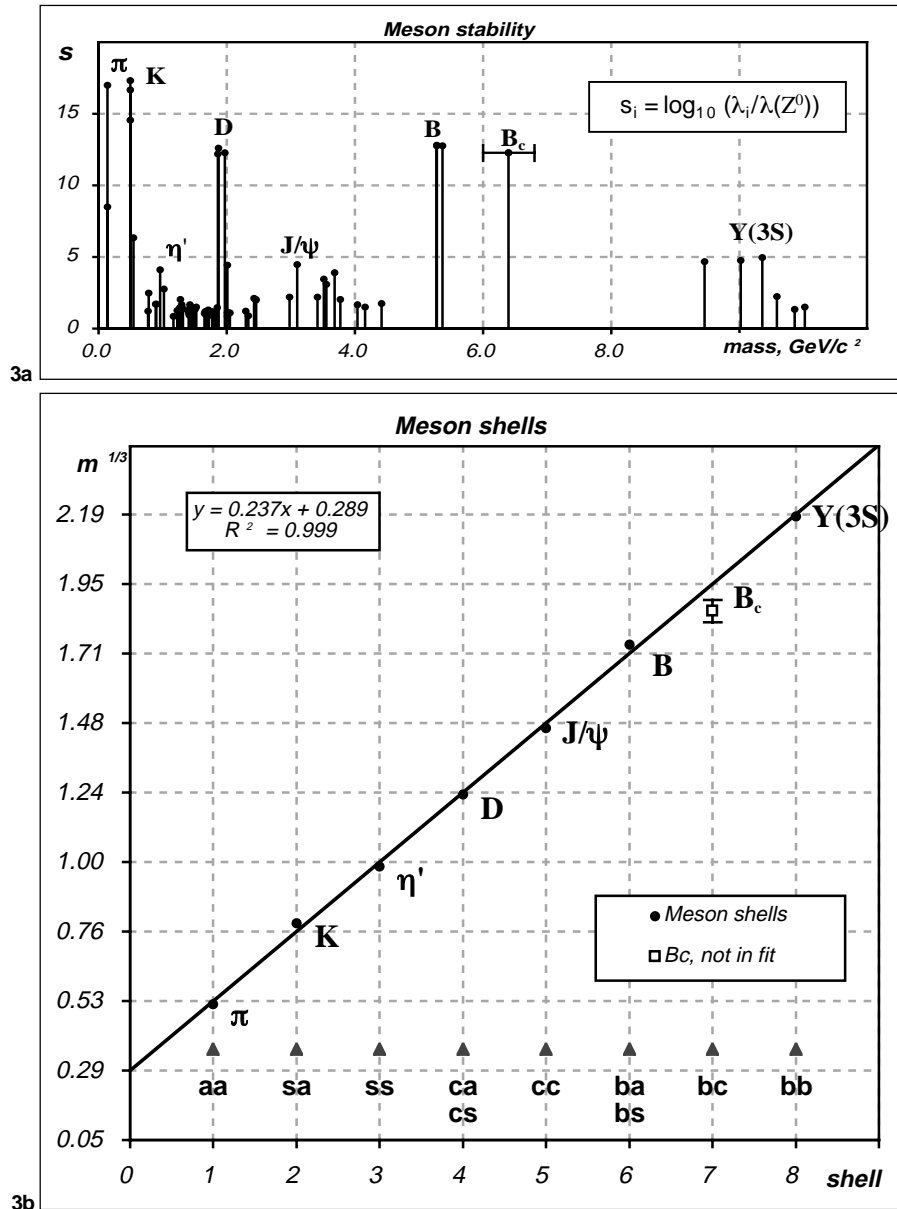


Fig. 3. Meson shells: 3a, meson stability plot, $s_i = \log_{10}(\lambda_i/\lambda(Z^0))$ vs mass, with evidence of meson shells 1 to 8; 3b, meson shells stability line fit with R^2 correlation parameter, and also quark composition for the various shells ($a = u \vee d$; $xy = xybar \vee yxbar$). Ad-hoc y scale

4. Meson shells and mass unit

The evidence for meson shells [1] is summarized in figure 3. For all mesons with known lifetime, a stability parameter s is charted against the mass (figure 3a) showing 8 outstanding stability peaks, and the cube root of their masses is plotted as a function of the serial number of the peak, interpreted as shell number (figure 3b). Assuming only that the mass is proportional to the number of constituents, the remarkable linear fit of the masses indicates that, at certain multiples of the unit mass, there are relatively stable structures – suggestive of an organization in shells.

This assumption is unusual. Furthermore it may be argued that the line fit is good, but not as sharp as the nuclear stability lines. The K and the B show positive residuals, and even by locating shell 8 at the $Y(1S)$ the R^2 of the fit does not improve (plot not shown). If mesons are really shell-structured, these deviations must be understood. On the other hand, it is interesting that the meson shell progression is correlated with the quark composition, as displayed in figure 3b. In this sequence the strange flavor plays a curious role that will be discussed further on in 6.1.

From the shells viewpoint, the quantization of the mass units for the various families (figure 2b) is probably related to structural features, therefore it may help understanding the organization of the bound states for the various meson types, and possibly also the origin of the residuals.

To proceed with this analysis, it is interesting to combine shells and mass unit, and convert the masses of the states on the meson stability line into number of partons using the values of P obtained from the mass multiplicity analysis [3]. Apart from the B_c in shell 7, this value is available for all other shells, yielding the following series and line parameters (plot not shown):

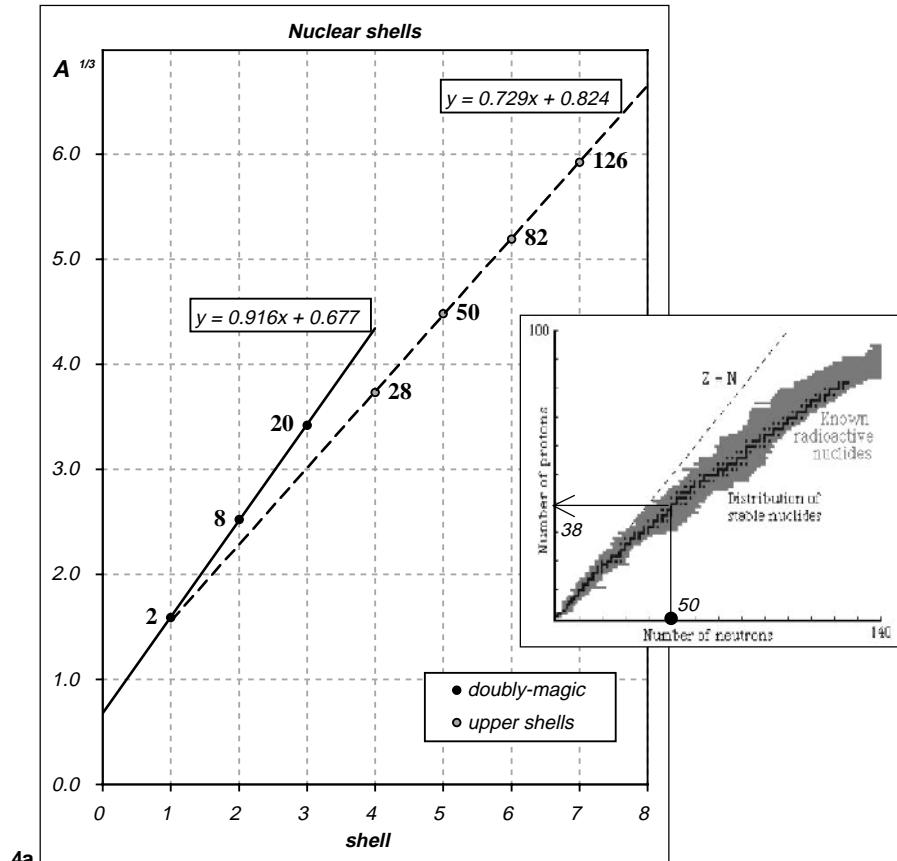
$$M(i): (4, 14, 28, 54, 84, 152, *, 294) [i=1,8], \quad y = 0.712 * x + 0.894, \quad R^2 = 0.9981$$

very similar to the corresponding values for the second nuclear line (figure 1b):

$$N(i): (4, 12, 28, 52, 88, 140, 208) [i=1,7], \quad y = 0.729 * x + 0.824, \quad R^2 = 0.9999$$

By converting masses to parton numbers (P), the R^2 of the fit did not improve, however the stability lines of the bound states under consideration express the aggregation of a finite number of constituents arranged in spherical or spheroidal shells, therefore the line parameters do not span a continuum and cannot assume just any possible value.

Being the series almost identical (at least for shells 1 to 5) with almost identical parameters, the underlying structure for both mesons and nuclei must also be similar. To understand this similarity, in the next page nuclear stability will be studied in more detail from this point of view.



4a

n	(n+1)*n	S1	N1	Z1	A1	S2	N2	Z2	A2	dA2
1	2	4	2	2	4	4	2	2	4	0
2	6	16	8	8	16	12	6	6	12	0
3	12	40	20	20	40	28	14	14	28	0
4	20	80				52	28	24	52	0
5	30	140				88	50	40	88	0
6	42	224				136	82	58	140	4
7	56	336				200	126	82	208	8
8	72	408				280				

4b

Fig. 4. The two nuclear stability lines: 4a, cube_root(A) versus shell number, the points are tagged with the values of the neutron number N corresponding to the magic series; 4b, table of N, Z, A versus shell number, for the nuclei on the two lines. A more detailed explanation is given in the text.

5. From the Segrè plot to nuclear stability lines

Nuclei are shell-structured – and so are atoms – and in both cases a spin-orbit interaction distorts the basic spherical symmetry. Figure 4 shows the two stability lines obtained in [1] by combining the neutron magic number sequence with the Segrè plot. The procedure is explained here in more detail: for each magic value of the neutron number

$$N(i): [i=1, 7] = 2, 8, 20, 28, 50, 82, 126$$

a corresponding value Z(i) is obtained by looking up the nucleus with neutron number equal to N(i) along the bottom of the mass-energy valley in the Segrè plot. The cube root of $A=N+Z$ is then plotted as a function of the shell number i, and the points are fitted with two straight lines.

The higher slope line (#1) fits shells 1, 2 and 3, and joins the points of the doubly-magic He-4, O-16 and Ca-40 in the low-A region where the stability valley follows the Z=N line. The lower slope line (#2) fits shells 4 to 7, where spin-orbit coupling is relevant and the valley bends towards a growing neutron excess. The two lines show interesting properties:

- they cross at the first shell, He-4 ($\delta y < 3\%$);
- in shells 2 and 3, line #2 corresponds to values of A of 12=6+6 and 28=14+14; 14 was recognized long ago as being quasi-magic, while the “magicity” of 6 is a more recent result [4];
- the ratio of the cubes of the slopes of the two lines is 1.99, very close to 2, indicating that the number of nucleons in series #2 grows from one shell to the next at a rate that is 1/2 the one of series #1

As explained in what follows, the values of A for lines #1 and #2 (columns A1 and A2 respectively in table 4b) can be expressed by the two series, also expanded in table 4b:

$$S1(n) = 2 * [\sum_{i=1}^n (i+1)^i, i=n, 1, 1] = 2 * [(n+1)*n + n*(n-1) + .. + 2*1]$$

$$S2(n) = 2 * [\sum_{i=1}^n (i+1)^i, i=n, 1, 2] = 2 * [(n+1)*n + (n-1)*(n-2) + ..]$$

For the doubly-magic stability line #1 and also for shells 1 to 5 of stability line #2 the experimental values A1 and A2 coincide with series S1 and S2 respectively. In shells 6 and 7 the experimental values of A2 are actually slightly larger than the S2 series by the amount $dA2=A2-S2$, 4 and 8 nucleons.

By comparison the values of P for the 8 meson shells obtained in the previous page exhibit larger residuals = (0, 2, 0, 2, -4, 12, *, 14). Which state to choose for shell 8 is debatable, but for shells 1 to 6 the choice with the stability plot is unambiguous, although near the J/ψ in shell 5 sits the η_c with P=88, the nominal value. It would seem that the basic volumetric stability progression is distorted by other effects, probably related to the different flavor combination of the dominant stable states in the various shells.

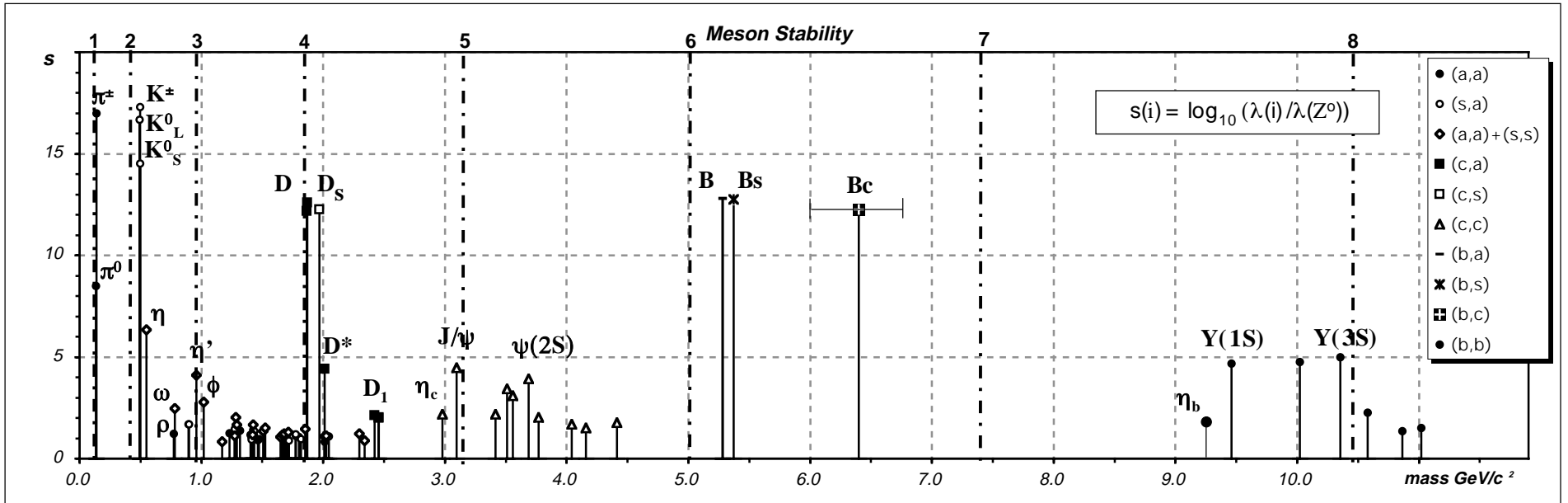


Fig. 5. Meson stability vs mass as in figure 6 of [1], mesons tagged with their flavor composition. Shell closure mass values computed from the fit of figure 3d, and marked with vertical dotted lines tagged with the shell number 1 to 8 above the chart margin, The sample consists of all the mesons in the PDG file [9] with defined width, plus the η_b .

6. Meson stability

The graph of meson stability versus the mass of figure 3a is expanded in figure 5. Here the mesons are tagged with their quark composition, a few more states are identified beyond those defining relative maximum stability, and the positions of the shells from 1 to 8, corresponding to the stability line fit of figure 3d, are shown on the plot.

6.1 The whole spectrum

After the first shell with the pions, the spectrum is empty up to shell 2, the kaons, and subsequent shells emerge after a gap of low-stability states and, apart from shell 3, correspond to a flavor combination never seen before, according to the series in the legend of figure 5. The **a** stands for **u** or **d**, and a concise notation is used so that, for example, **(c,a)** stands for **c-dbar** or **c-ubar** or **cbar-u** or **cbar-d**. Shell 1 starts with unflavored mesons without hidden strangeness **(a,a)**, shell 2 with strange mesons **(s,a)**, shell 3 with **(s,s)**, shell 4 with **(c,a)** (and **(c,s)** nearby), shell 5 with **(c,c)** and so on.

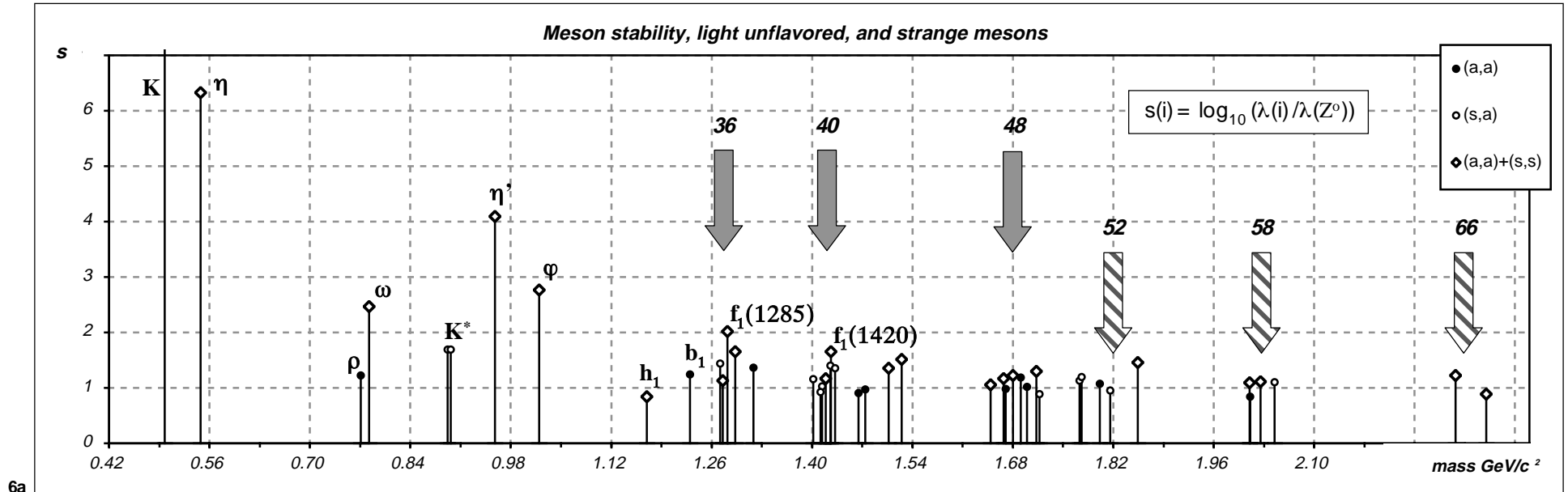
The strange flavor plays an intriguing double role: combined with an **a** it starts shell 2, as **(s,s)** it starts shell 3, while in shells 4 and 6 it acts as a modifier

replacing an **a** just 2 or 4 mass units above shell inception. Consistent with this pattern, it shows up also ahead of time after the start of shell 2, where the η — the lowest mass state with hidden strangeness — is at $P=16$, just 2 units above the K with $P=14$.

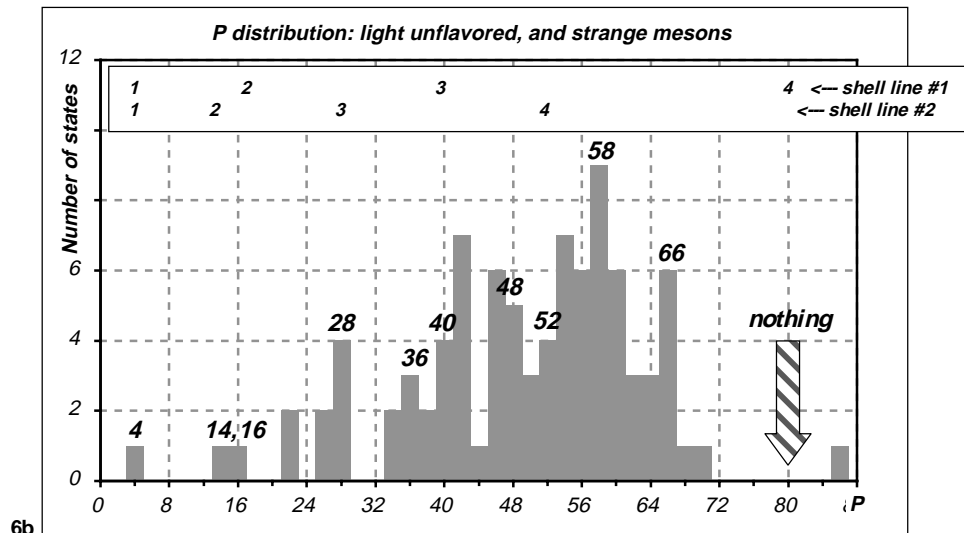
In shells 1, 2 and 4, stability falls rapidly from above 12 at shell closure down to less than 2, and in the first 3 shells several low-stability states with the same flavor tag are present at masses above the subsequent shells. In the **x-xbar** shells 3, 5 and 8 the shell closure stability value is around 5 and falls more gently. The mass range of the first three shells and their tails will be expanded in the next page.

As already noted, the K in shell 2 deviates from the meson stability line of figure 3d, being at $P=14$ rather than 12 and so does the D at $P=54$ instead of 52. The deviation of the B is more substantial ($dP=12$), while the B_c has a large error on the mass and is not used in the fit.

By analogy with previous **(x,xbar)** shells, it would seem more appropriate to choose the Y(1S) rather than the Y(3S) as shell inception, although both choices deviate from the nominal value of P. Notice the η_b at $9.3 \text{ GeV}/c^2$ (lifetime not measured) and the pairs (η', ϕ) , $(\eta_c, J/\psi)$, $(\eta_b, Y(1S))$.



6a



6b

Fig. 6. Light unflavored mesons and strange mesons: 6a, meson stability vs mass with scale in steps of $70 \text{ MeV}/c^2$ and meson clusters identified by block arrows; 6b, histogram of P for all states used in the analysis of reference [3], including all f mesons with known P . The range around $P=80$, corresponding to shell 4 in shell line #1 is empty.

6.2 Light unflavored mesons and strange mesons

Part of the full mass range of figure 5 is expanded in figure 6a, with the mass scale in steps of $70 \text{ MeV}/c^2$. The plot shows three clusters around $1260 \text{ MeV}/c^2$ ($P=36$), $1420 \text{ MeV}/c^2$ ($P=40$), and $1680 \text{ MeV}/c^2$ ($P=48$). Three more clusters with fewer states are visible, at approximately $1820 \text{ MeV}/c^2$ ($P=52$), $2030 \text{ MeV}/c^2$ ($P=58$), and $2310 \text{ MeV}/c^2$ ($P=66$). The configuration with $P=40$ corresponds to the third shell in the nuclear line #1, analogous to the doubly-magic Ca-40.

The distribution of P for all (a,a), (s,a) and (s,s) states retained for the mass analysis of [3], including also all f mesons for which P can be evaluated, is shown in figure 6b, and confirms the three clusters around 36, 40 and 48, as well as at 52, 58 and 66. Some peaks appear shifted by a δP of 2, but figure 6b shows states population density irrespective of stability.

Shell 4 in the doubly-magic-equivalent series is at $2800 \text{ MeV}/c^2$ ($P=80$), and the histogram 6b is empty from 72 to 84. The heaviest (a,a) or (s,s) meson listed in the regular summary table of the PDG is the $f_6(2510)$, while the "further states" section carries an unidentified $X(2750)$ and two more such states at 3250. No D or D_s states are known around that mass value either. The state at $P=86$ is the $K(3100)$. As in nuclei, the doubly-magic-equivalent shell series stops at 3.

In the shell interpretation the peaks at $P=36, 48, 52, 58$ and 56 would correspond to sub-shell configurations, and their precise understanding requires a more advanced model, not available at the present time.

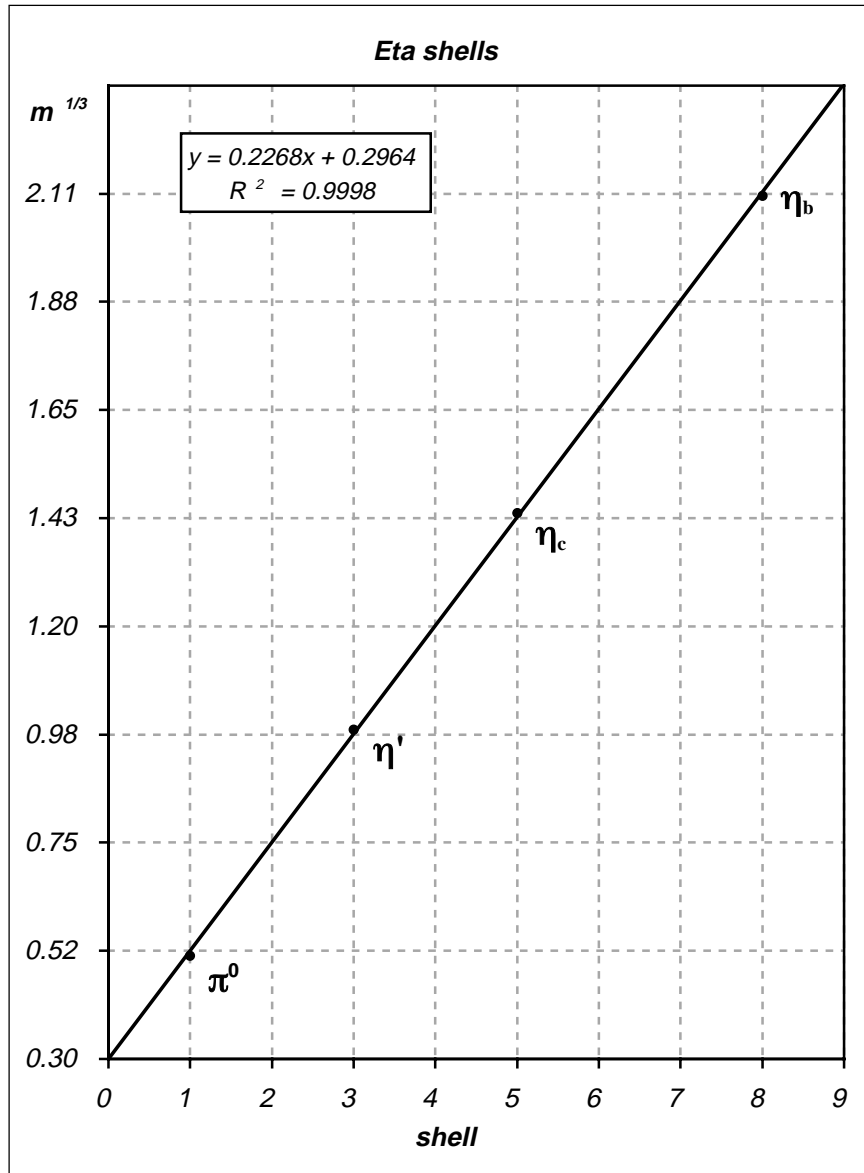


Fig. 7. Eta shells. Mass stability line $\text{cube_root}(m)$ vs shell number, with π^0 , η' , η_c and η_b in shells 1,3, 5 and 8, showing a superior alignment compared with the original meson shells mass stability line. Ad-hoc vertical scale. The motivation for this plot is explained in the text.

7. U-grid, FCC lattice and η shells

The mass patterns in the meson spectrum – with a fixed mass contribution for each parton – are suggestive of solid-phase aggregates, possibly a 3D lattice organization. If so, the quantization of the mass unit on a grid of 13 values, as seen in figure 2b, might be related to the coordination number of the lattice itself.

With spins and charges equal or close to 0, and the large number of partons, the meson aggregates must be organized with alternating up/down spins and +/- charges. On a periodic lattice with coordination number = 12 (such as the FCC*), with spin-1/2 partons of charge 0, -1 and +1, arranged as a partially charged "ionic" lattice, several configurations are possible [5]. For a given node of the lattice, the number of charged neighbors k can vary from 0 (all neutral) to 12 (all charged), a total of 13 values. Depending on the charge balancing constraints on these lattice variants, some values of k may not be realized, while other may correspond to more than one configuration, as seen in figure 2b (a more detailed model will be described in a separate article, here only selected structural properties are discussed). Charge balancing constraints might be the reason for the deviation of the value of P of the shell states from series S2.

Assuming that the contribution to the total mass is larger for a charged parton than for a neutral one, then $u(0) = 33.88 \text{ MeV}/c^2$ in figure 2b is the contribution of a neutral parton, and $u(12) = 36.84 \text{ MeV}/c^2$ the charged one. This assumption agrees with the charges of the final products of the decays of the μ (1 charged out of 3 = 4/12, $k=4$) and of the π^\pm (1 charged out of 4 = 3/12, $k=3$) as verified by the position of the corresponding points on the u -grid of figure 2b. This would not be true with the neutral parton heavier than the charged one.

On the u -grid both the η and the η_c sit at $k=0$, with all constituents neutral [5]. The specific mass unit of the π^0 is 33.74, close to $u(0) = 33.88$, so that 4 neutral constituents can be assumed [5]. The pion is at shell 1 with $P=4$, while the η' is at shell 3 with $P=28$, and the η_c at shell 5 with $P=88$, right at the nominal values of P as defined by series S2 in table 4b. With no charged constituents, the η and η_c do not need to obey any charge balancing constraints and can sit right at the geometrical shell closure. Considering that this should also be true for the η_b , it is expected that the mass stability line with the π^0 , η' , η_c and η_b in shells 1, 3, 5 and 8 would show a sharper alignment compared to the stability line of figure 3a. This is indeed verified by the chart in figure 7, which confirms the conjecture.

Mesons are similar to nuclei and at the same time show indications of a solid-phase FCC structure, and this may be more than a coincidence. FCC nuclei are not new, and appendix A is a summary of an interesting but little known FCC model of the atomic nucleus, showing also the derivation of the series S1 and S2.

* The HCP lattice also has coordination number = 12, but it is not considered, as it does not conduct to the geometrical derivation of the S1 and S2 shell series that are relevant for nuclei and mesons (see appendix A).

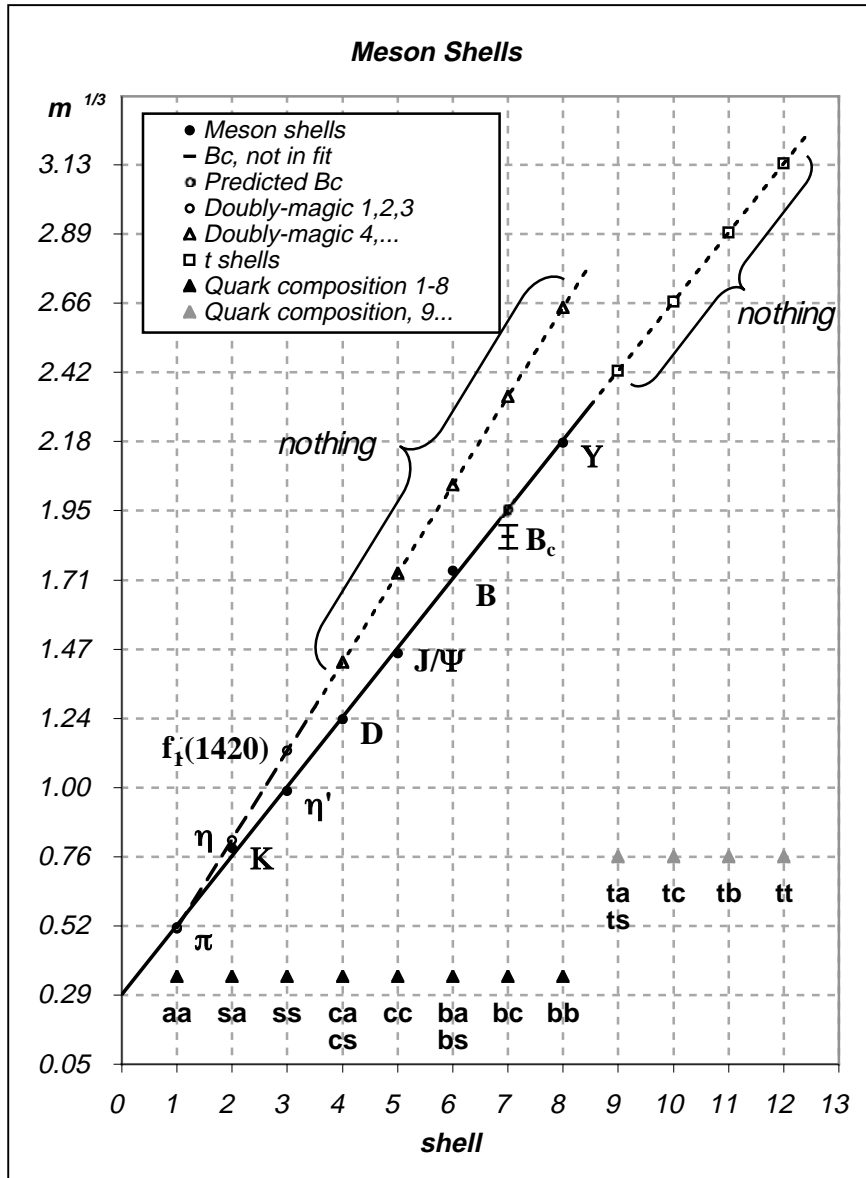


Fig. 8. Meson shells organization, showing two stability lines, extrapolated mass values for subsequent shells where no know particle has been found, and quark composition progression for the main sequence. Ad-hoc vertical scale corresponding to the main shell progression.

8. Meson shells, the full picture

The sharp η shells plot with the related u-grid interpretation are encouraging, and indicate that the residuals of the meson stability line are due to second-order charge-balancing effects which distort the basic $\text{cube_root}(P)$ shell arrangement. Although these indications could only be proven correct by a complete model, they strengthen the original shell evidence considerably. Further confirmation is provided by the clustering of states in the low-mass segment of the meson stability plot, a sign of sub-shells.

The complete meson shells organization is resumed in figure 8, showing what is there and also what is not:

- along the original mass stability line from shell 1 to shell 8, also the equivalent of the nuclear doubly-magic shells can be identified; apart from the pion common to both lines, like the He-4 in the nuclear shells plot, the η at P=16 is the equivalent of O-16 for shell 2, while a cluster of states centered at P=40, with the $f_1(1420)$ as the most stable state, corresponds to Ca-40 for shell 3.
- no states are known near the extrapolated mass values for the following shells in that series, yet another confirmation of the mesons-nuclei analogy;
- of special interest is the pion-He-4 correspondence, characterizing the pion as the equivalent of the nuclear alpha-particle;
- on the main lower-slope meson stability line, the quark composition progression from shell 1 to 8 is:

aa, sa, ss, ca+cs, cc, ba+bs, bc, bb ;

apart from the intriguing role of the s quark, in first approximation the sequence and the plot account for the values of the quark masses as listed in the PDG, if quarks are interpreted as constituents rather than simply as valence properties, and are coupled with positive binding energy; in fact this is a kind of explanation of the mysterious spectrum of quark masses, for whatever it is worth; needless to say, the exercise with binding energies is a tricky one already for the few states in the shell plot, not to mention the rest of the spectrum;

- if there were a t quark, then by extrapolating the sequence of the shell q-qbar content 4 more shells would be expected at specific mass values in the range 14 - 31 GeV/c² while none has been observed; it might well be that shell 8 is just the structural limit for this kind of bound states, like 6 for atoms and 7 or 8 for nuclei; if so, what are the top events from FNAL? and what about the quark-lepton correspondence?

9. Summary of results

The analysis developed in this article started from previous indications [1] that:

- baryons and mesons are structured in shells, and their shell organization is different;

and transformed the meson shell pattern using the mass unit results [3], i.e.:

- particle masses below $1 \text{ GeV}/c^2$ are integer multiples P of a mass unit u of about $35 \text{ MeV}/c^2$, odd for fermions and even for bosons: $m = P \cdot u$
- the periodicity restricted to mesons of the same family extends to the whole spectrum;
- mass units of all analyzed meson families are distributed on a u -grid of 13 values spaced by about $0.25 \text{ MeV}/c^2$, with locations on the grid strongly correlated with J^{PC} and the quark composition.

Interpreting P as the number of partons, it has been deduced that:

- a) the shell organization of mesons is similar to that of nuclei, i.e.:
 - almost identical population of constituents in the various shells (up to shell 5 inclusive);
 - same pattern of 2 stability lines, doubly magic-equivalent extending only up to shell 3;
- b) the main shell progression is correlated with the quark composition and no states are present at the expected mass values of the hypothetical t -shells 9, 10, ...;
- c) the meson mass spectrum patterns are compatible with solid-phase bound states on an FCC lattice, with anti-parallel spin coupling and $+1/-1$ charge distribution in various degrees of partial filling, from $0/12$ to $12/12$, in agreement with the u -grid;
- d) the shell sequence ($1=\pi^0$, $3=\eta'$, $5=\eta_c$, $8=\eta_b$) shows a sharper alignment, consistent with (c) and the position of those states on the u -grid at $u(0)$;
- e) the progression of the q - q -bar content of the meson shells offers a rationale for the mysterious estimated values of the quark masses;
- f) the masses of the unstable leptons μ and τ are part of the same multiplicity scheme, but with odd values of P ; their mass unit at $u(4)$ agrees with the interpretation of point (c).
- g) the FCC lattice indications for the mesons and the shell pattern similarity with nuclei reinforce the relevance of the FCC nuclear model.

10. Discussion

Meson shells and mass unit combined reveal features of the mesonic structure that are surprising in the light of the current understanding of quarks. On the other hand, the meson mass patterns are solid experimental results that extend previously observed multiplicity indications to the whole spectrum. The masses of the mesons defining the shells, expressed with the number of partons obtained from the multiplicity analysis, turn into an integer series almost identical to that of the nuclear shells. A detailed analysis of the stability landscape shows evidence of a second shell line, and also indications of sub-shells. The geometric similarity with nuclei is striking.

Further structural properties are deduced from the u -grid, the set of discrete values of the mass unit. The u -grid quantization has a p -value of 0.95, moreover the correlations with J^{PC} and the quark composition are outstanding. The puzzling sequence of the quark masses can be understood (with the exclusion of the top) from the cubic shell progression and the quark composition of shells 1 to 8, while the range of discrete values of the mass unit on the u -grid promises further insight into the real meaning of the quarks. The span of the u -grid is related to the FCC lattice through a simple charge composition hypothesis, confirmed by selected decay modes and also by the sharper shell line of the η -like states. Finally, the nuclear analogy and the FCC lattice, derived from experimental evidence, resonate with the FCC nuclear model.

These results, incompatible with current assumptions on the structure of particles, are statistically sound and logically compelling, and cannot be attributed to a coincidence. Following the strategy outlined in the introduction, their implications will be carried forward, and conclusions drawn only at the end. How comes that all this was not seen or considered before? As explained in the brief history of the particle mass multiplicity in reference [3], this concept is not new. Apparently the mass, a fundamental physical quantity that theory cannot predict, is no longer considered important and is used mostly as a tag to identify states. In the PDG the mass of several states is "estimated based on the observed range of the data and without a formal statistical procedure", and from the mass unit fits [3] there is evidence that in many cases the errors on the mass quoted by the experiments are sometimes overestimated.

Compared to what was previously known, the mass unit evidence from [3] revisited here is more systematic and considerably reinforced by the shell organization, and also by the nuclear analogy and the FCC indications from the u -grid. A detailed model is being developed and will be published separately, but a number of its ingredients can already be formulated and compared with the properties of the standard model.

10.1 Ingredients for a model of mesons

1. mesons are spheroidal partonic structures on an FCC lattice, made of an even number of spin 1/2 partons (and antipartons) of charge 0, +1 and -1,
 2. spins are arranged anti-ferromagnetically and charges are alternating in various charge configurations related to the quark composition;
 3. the average total contribution of each neutral and charged parton to the meson mass is 33.88 and 36.84 MeV/c² respectively [5];
 4. relative stability is maximal nearby geometric shell closures defined by the FCC series S1 (shells 1 to 3) and S2 (shells 1 to 8);
 5. with two, possibly three, different kinds of mesons located at position u(0) on the u-grid, there must be more than one kind of neutral partons;
 6. all mesons are unstable, therefore the quantum-mechanical binding is realized with positive binding energy;
 7. from points 3 and 6 it appears that the masses of the free partons are quite small, less than their effective mass in the bound state as from point 3;
 8. decays and interactions proceed through fragmentation and recombination of the bound states, possibly with parton-antiparton annihilation and pair creation;
 9. given the geometrical arrangement on the lattice, there is no need for color;
 10. with partons on the nodes of a lattice, rotational degrees of freedom are not present, and in first approximation there is no dynamics in the bound state;
- ... and more to be derived from the baryon analysis.

Looking for neutral and charged partons and antipartons with spin 1/2 and mass less than 30 MeV/c², and with more than one type of neutrals, among the known particles there is only one possible choice: the stable leptons. A model of particles with stable leptons as constituents has been proposed by A. O. Barut [10], and several aspects of his work might be a good source of inspiration. Isospin and strangeness are derived as structural properties and so is the SU(3) symmetry; an energy scale of $m_e/\alpha = 70 \text{ MeV}/c^2$ is associated with unstable magnetic resonances of two spin-1/2 particles with positive binding energy; a mechanism for CP violation is derived; a model for the nucleus can be formulated, such that lattice structure and gas behavior coexist, solving the problem of the nucleon mean free path.

In the model being developed here, up to now one discrepancy with the data is outstanding: the q-qbar progression breaks down after mesonic shell 8, therefore the interpretation of the top events from FNAL does not fit this scheme.

10.2 Beyond the standard model?

The standard model of particle physics is a conubium of a solid theory of electro-weak interactions and a less convincing strong sector. Apart from the difficulties in predicting particle masses, a conceptual problem with this formulation is that, although the model is incomplete, it requires a large number of fundamental constants, 26 if not more. Many of these constants would become redundant in the eventuality that the present line of research – which is just at the beginning and where a lot remains to be done – ended up being successful:

- quarks are valence properties, so their masses are not defined (-6);
- the W-quark couplings are derived from the expression of the quarks in terms of the constituents (-4);
- the muon and the tau leptons are composite, their mass is computed (-2);
- strong interactions are a collective manifestation of electromagnetism, and the strong coupling constant can be computed (-1).

In this way at least 13 parameters, half of the total, would no longer be necessary, and the overall picture of particle physics would be considerably simplified. Seen from this perspective, particle interactions lose some of their glamour, and are reduced to a kind of peculiar ballistic crystallography, while the structure of leptons becomes the new frontier. In the same way, with particles as bound states of leptons and anti-leptons, the matter-antimatter asymmetry problem shifts from the scale of the universe down to the level of the atom.

The problems and limitations of the standard model have led particle theorists to develop various extensions of it, such as super-symmetric theories, GUTs or theories with extra space dimensions. This line of thinking started in the early 80's and by now at almost any particle physics conference, meeting or school the slogan "beyond the standard model" is seen over and over again.

When Copernicus centered, for good reasons, the circular orbits of the planets on the sun, to fit the data he needed more epicycles than Ptolemy. After all, he wanted to build a more symmetric theory. Kepler had more precise data, and for years he tried to fit them using epicycles within epicycles, and failed. Finally he gave up symmetry, tried elliptic orbits and discovered the famous three laws of planetary motion that helped Newton formulate the law of gravitation. Dozens of parameters were reduced to one, and nothing was left of the original theory.

Is "beyond the standard model" the way to go?

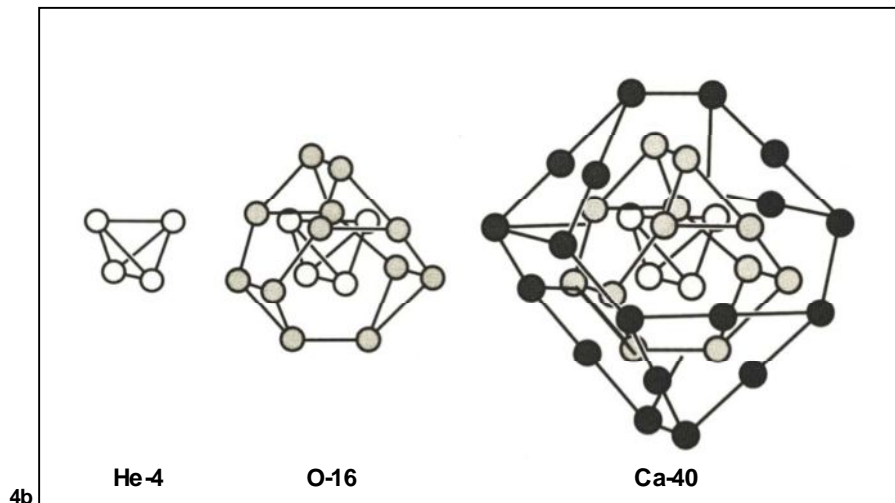
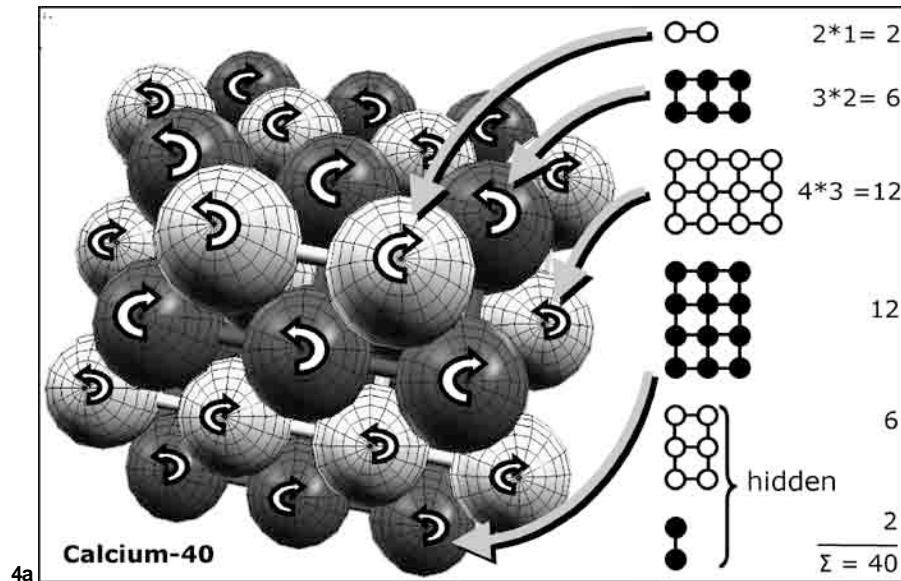


Fig. 9. FCC nuclei: 9a, Ca-40 with alternating layers of protons and neutrons in black and white, and anti-ferromagnetic spin arrangement in each layer (adapted from NVS [8]; the picture is to scale and the nucleon radius in the drawing is the charge radius); 9b, the first three doubly-magic nuclei: He-4, O-16, Ca-40; the nucleons of the first, second, third shell are colored in white, gray, black.

Appendix A. The FCC nuclear model

The obvious tool to understand the similarity between mesonic and nuclear shells would seem to be the nuclear IP model, evolution of the original spin-orbit coupling shell model of Mayer and Jensen. In spite of its shortcomings and inconsistencies, it still is the prevalent theoretical paradigm in nuclear physics. Actually, given the FCC lattice indications from the meson spectrum, there may be a better choice: the FCC model of Cook and Dallacasa [6].

Lattice models are used in nuclear physics in multi-fragmentation simulations (see for example [7]), and for convenience the simple cubic lattice has been the most frequently used. Several studies have found that the FCC lattice reproduces the experimental distributions of fragment masses and their energy spectra more accurately. Still, in mainstream nuclear physics, lattices are employed as computational techniques rather than as formal models.

In the face-centered-cubic (FCC) model of the nucleus by N. D. Cook and V. Dallacasa [6], the nucleons are located at the nodes of an FCC lattice, with alternating neutron and proton layers arranged anti-ferromagnetically in a chessboard pattern, so that nearest neighbors in any layer have opposite spins. The interaction is short-range.

The FCC model unifies shell, liquid-drop and cluster properties, as found in the conventional models, within a single theoretical framework, and solves the controversial issues of nuclear orbiting and the range of the nuclear force. At the same time it is fully compatible with the IP model and it reproduces the sequence of allowed nucleon states, with the same shells and sub-shells patterns [6].

For the scope of the present work, the FCC model provides a simple geometrical algorithm to compute the total number of nucleons in full shell configurations and sub-shells, and permits a direct geometrical interpretation of the two nuclear stability lines. The nucleus corresponding to the n th full shell (upper stability line) is built starting from an XY lattice layer of size $(n+1)*n$, adding on top of it the $n*(n-1)$, and so on up to $2*1$. At the bottom the same structure is mirrored, rotated by 90° around the Z axis. For example, the (20,20) doubly magic Ca-40 of shell 3 consists of a layer of $4*3$ nucleons, with a $3*2$ layer and a $2*1$ layer on top, and the 90° -rotated mirror ziggurat below, for a total of $2*(12+6+2) = 40$ nucleons (figure 9a).

The nucleus of the n th shell on the lower slope line is obtained simply by starting from the same XY lattice trellis of size $(n+1)*n$ and adding one out of two of the layers used in the full expansion for the doubly-magic. These two geometric progressions define the series S1 and S2 mentioned in section 5. The NVS package [8] helps visualizing various properties of the FCC nuclear states.

Appendix B Data and Statistics

Particle masses and lifetimes were taken from the 2002 PDG RPP [9]. The least-squares fits are performed and charted with MS Excel. The correlation coefficient R^2 is the square of Pearson's product moment correlation R:

$$R = \frac{n(\sum xy) - (\sum x)(\sum y)}{\sqrt{((n\sum x^2) - (\sum x)^2)(n\sum y^2) - (\sum y)^2}}$$

It expresses the fraction of the total variation of the sample $\{(x_i, y_i), i=1, n\}$, that is accounted for by the least-squares regression line, and it varies from 1 (perfect linear correlation) to 0 (no correlation).

The p-value quantifies the goodness-of-fit of the data to a hypothesis. For the mass multiplicity fits, it is defined as the probability to find R^2 in the region between 0 and the value observed with the data. It is computed for each fit by Montecarlo simulation, with the procedure described in reference [3].

Bibliography

- [1] P. Palazzi, *Partides and Shells*, CERN-OPEN-2003-006 (2003), <<http://cdsweb.cern.ch/search.py?recid=602200&ln=en>>, also at <<http://arxiv.org/abs/physics/0301074>>
- [2] Y. Nambu, *An Empirical Mass Spectrum of Elementary Partides*, Prog. Theor. Phys. **7**, 131 (1952).
- [3] P. Palazzi, *Patterns in the Meson Mass Spectrum*, p3a-2004-001 (2004), <<http://particlez.org/p3a/abstract/2004-001.html>>
- [4] C. Samanta and D. Adhikari, *New Magicity in Light Nuclei* (2001) <<http://arxiv.org/pdf/nucl-th/0105014>>
- [5] S. Giani, *Particle Masses below 1 GeV/c²*, in preparation.
- [6] N. D. Cook and V. Dallacasa, *Face-centered-cubic solid-phase theory of the nucleus*, Phys. Rev. **C35**, 1883 (1987)
- [7] G. Musulmanbekov, A. Al-Haidary, *Fragmentation of Nuclei at Intermediate and High Energies in Modified Cascade Model*, (2002) <<http://arxiv.org/abs/nucl-th/0206054>>
- [8] N. D. Cook, *NVS - Nuclear Visualization Software*, <<http://www.res.kut.ac.jp/~cook/NVSIndex.html?>>
- [9] PDG, *Masses, Widths, and MC ID Numbers from 2002 edition of RPP*, (2002), <http://pdg.lbl.gov/rpp/mcdata/mass_width_02.mc>
- [10] A. O. Barut, *Stable Partides as Building Blocks of Matter*, Surveys High.Energ.Phys. 1:113 (1980)

Acknowledgements

Norman Cook introduced me to the FCC nuclear model providing copies of his papers, notes and software, and answered many questions by e-mail.

Simone Giani shared his insight on particle mass regularities and statistical aspects of the analysis during many late evening discussions.

Malcolm Mac Gregor answered numerous queries and encouraged this work through a substantial e-mail exchange.

Norman Cook, Simone Giani and Simone Gilardoni reviewed the draft and suggested various improvements.

To all the people mentioned above I am very grateful.

Revision Record

- 01-MAR-2005 preprint, original electronic submission, published on the independent electronic Particle Physics Preprint Archive p3a;
- 13-MAR-2005 revision 1:
abstract simplified; section 6.2 and figure 6b upgraded with more states; minor language and plot formatting improvements.

Set in Helvetica and Symbol, formatted with PowerPoint and embedded Excel plots on an Apple Macintosh PowerBook Ti running MacOSX.